Matrix Metalloproteinase-2 Activated by Ultraviolet-B Degrades Human Ciliary Zonules *In Vitro*

Yuki Shiroto[1], Ryo Saga[1], Hironori Yoshino[1], Yoichiro Hosokawa[1], Keitaro Isokawa[2] and Eichi Tsuruga[1]

[1]Department of Radiation Science, Graduate School of Health Sciences, Hirosaki University, 66–1 Honcho, Hirosaki, Aomori 036–8564, Japan and [2]Department of Anatomy, Nihon University School of Dentistry, 1–8–13, Kanda-Surugadai, Chiyoda-ku, Tokyo 101–8310, Japan

The ciliary zonules, also known as the zonules of Zinn, help to control the thickness of the lens during focusing. The ciliary zonules are composed of oxytalan fibers, which are synthesized by human nonpigmented ciliary epithelial cells (HNPCEC). The ciliary zonules are exposed to ultraviolet (UV), especially UV-A and UV-B, throughout life. We previously demonstrated that UV-B, but not UV-A, degrades fibrillin-1- and fibrillin-2-positive oxytalan fibers. However, the mechanism by which UV-B degrades oxytalan fibers remains unknown. In this study, we investigate the involvement of matrix metalloproteinase-2 (MMP-2) in the UV-B-induced degradation of fibrillin-1- and fibrillin-2-positive oxytalan fibers in cultured HNPCECs. Enzyme-linked immunosorbent assay revealed that UV-B irradiation at levels of 100 and 150 mJ/cm^2 significantly increased the level of active MMP-2. Notably, MMP-2 inhibitors completely suppressed the degradation of fibrillin-1- and fibrillin-2-positive oxytalan fibers. In addition, we show that UV-B activates MMP-2 via stress-responsive kinase p38. Taken together, the results suggest that UV-B activates a production of active type of MMP-2 via the p38 pathway, and subsequently, an active-type MMP-2 degrades the fibrillin-1- and fibrillin-2-positive oxytalan fibers in cultured HNPCECs.

Key words: ciliary zonule, fibrillin, ultraviolet-B, matrix metalloproteinase-2, p38

I. Introduction

Elastic system fibers, as well as collagen fibers, form the extracellular matrix and comprise oxytalan, elaunin, and elastic fibers, which depend on the relative ultrastructural proportion of microfibril and elastin [15]. Oxytalan fibers are composed of bundles of closely joined parallel microfibrils with no elastin. The microfibrils mainly consist of fibrillin-1 and fibrillin-2, and other minor microfibril-associated molecules. Fibrillin-1 is ubiquitously distributed in the extracellular space [29], while fibrillin-2 is restricted to elastic fibers [28]. Human elastic tissues contain a com-

plex system of components such as oxytalan, elaunin, and elastic fibers, while pure oxytalan fibers are found in the ciliary zonules and periodontal ligaments [5, 18]. These components tend to degrade as an individual ages; however, the extent of the changes that occur in the elastic tissues with aging and the mechanisms of degradation remain unclear.

In the eye, the ciliary zonule links the ciliary body with the lens. It helps to control the thickness of the lens through its elasticity, which is necessary for transmitting force. A recent clinical topic of the ciliary body and the lens has been focused on the intraocular lens dislocation caused by weakening of the ciliary zonule [12]. However, a mechanism of the degradation of the ciliary zonule remains unsolved. Nonpigmented ciliary epithelial cells (NPCEC) in the ciliary body express fibrilin-1 and fibrillin-2, which

Correspondence to: Eichi Tsuruga, Department of Radiation Science, Graduate School of Health Sciences, Hirosaki University, 66–1 Honcho, Hirosaki, Aomori 036–8564, Japan. E-mail: tsuru@hirosaki.ac.jp

form bundles of microfibrils to create the ciliary zonule. Human ciliary zonule contains fibrillin-1 and fibrillin-2 and the other microfibril-associated molecules, such as microfibril-associated glycoprotein-1, latent transforming growth factor-β-binding protein-2, and elastin-microfibril interface localized protein 1 (EMILIN-1) [4]. The ciliary zonules are structurally exposed to ultraviolet (UV) throughout life [22]. UV-B (290–320 nm) penetrates to the planetary surface and is therefore a potent toxic agent. The exposure of the human ciliary zonule to UV-B weakens their elasticity and dissociates them, causing it to dislocate from the lens. Researchers also speculated that UV-B stimulates proteolysis of the ciliary zonule. Recently, we demonstrated that UV-B irradiation leads to the disappearance of oxytalan fibers positive for fibrillin-1 and fibrillin-2 in NPCEC culture [25]. Also, we showed previously that activated matrix metalloproteinase-2 (MMP-2) degrades fibrillin-1 and fibrillin-2 in the human periodontal fibroblast culture system [11]. Fibrillin-1 and fibrillin-2 are both substrates of MMP-2 [1, 7]. Therefore, in this study, we examine whether MMP-2 contributes to the degradation of fibrillin-1 and fibrillin-2 after UV-B irradiation in NPCEC culture.

II.   Materials and Methods

Cells and culture

HNPCECs were purchased from Science Cell Research Laboratories (Carlsbad, CA, USA) and cultured in Dulbecco's modified Eagle medium (DMEM; Sigma-Aldrich, St. Louis, MO, USA) supplemented with 10% newborn calf serum (Invitrogen, Grand Island, NY, USA), 100 U/mL penicillin, and 100 μg/mL streptomycin (Roche Diagnostics, Mannheim, Germany) at 37°C in a humidified atmosphere containing 5% CO_2. After the cells reached confluence, they were harvested with 0.025% trypsin (Invitrogen) in phosphate-buffered saline (PBS) and transferred to plastic culture dishes at a 1:4 split ratio. For experiments, the cells were trypsinized and seeded at a concentration of 1×10^6 cells/mL in 35-mm and 60-mm culture dishes (Corning Inc., Corning, NY, USA). For immunofluorescence analysis, the 35-mm culture dishes were used, and the 60-mm culture dishes were used for ELISA assay and Western blotting. HNPCECs reached confluence after 72 hr (set as day 0). The HNPCECs from three different donors were used after the third to sixth passages in this study.

UV irradiation

During the culture process after day 0, the medium was refreshed every 3 days. At 4 weeks of culture, the culture medium was removed, and the cells were washed twice with PBS. Then, the medium was replaced with PBS to avoid any photosensitization effect of the medium components, and UV irradiation was performed. The cells were irradiated with UV-B at levels of 0, 50, 100, and 150 mJ/cm^2 using a DNA-FIX (DF-312; ATTO, Tokyo, Japan),

as previously described [16]. The duration of UV-B irradiation to obtain a dose of 50 mJ/cm^2 was approximately 15 sec. The distance from the UV lamp to the cell culture dish was 145 mm. After irradiation, the cells were cultured for another 24 hours under the same culture conditions. Then, the cells were subjected to immunofluorescence analysis.

In some experiments, immediately after the irradiation of UV-B, the cultures were supplemented with 1.5 μM of MMP-2 inhibitor (APR-100; R&D Systems, Minneapolis, MN) or 50 nM MMP-2/MMP-9 inhibitor (MMP-2/MMP-9 Inhibitor I; EMD Millipore Corp., Billerica, MA, USA). A stock solution of both MMP inhibitors was dissolved in dimethyl sulfoxide (DMSO) and subsequently diluted with DMEM. The concentration of MMP-2 inhibitor and MMP-2/MMP-9 inhibitor employed was previously determined in earlier culture experiments [3, 21]. Control cultures contained an equivalent concentration (0.01%) of DMSO in DMEM, instead of MMP-inhibitors.

Also, in some experiments, the cells were seeded at 1×10^6 cells/mL in 35-mm and 60-mm culture dishes. After 24 hr, the cells were irradiated with UV-B, and then the cultures were supplemented with 2 μM of p38 inhibitor (SB203580; Cell Signaling Technology, Danvers, MA, USA). A stock solution of p38 inhibitor was dissolved in DMSO and subsequently diluted with DMEM. The concentration of p38 inhibitor used was previously determined in earlier culture experiments [9]. Control cultures contained an equivalent concentration (0.01%) of DMSO in DMEM, instead of p38 inhibitor.

Immunofluorescence

HNPCEC were fixed in ice-cold 4% paraformaldehyde in PBS for 15 min and then washed with PBS. Nonspecific immunoreactivity was blocked with 1% goat serum (Sigma, St. Louis, MO, USA) in PBS for 1 hr at room temperature. Then, the cell/matrix layers were incubated for 2 hr at room temperature with the appropriate primary antibodies (clone 11C1.3, monoclonal antibody against mouse fibrillin-1 diluted 1:1000 [Thermo Fisher Scientific, Fremont, CA, USA]; rabbit antibody against human fibrillin-2 diluted 1:1000 [Elastin Products Co., Owensville, MO, USA]). The monoclonal antibody against mouse fibrillin-1 reacts with human fibrillin-1 [2]. Controls were incubated with pre-immune normal mouse or rabbit IgG instead of the primary antibody. After being rinsed in PBS, the cells were incubated with Alexa Fluor 488-labeled goat anti-mouse IgG antibody or Alexa Fluor 568-labeled goat anti-rabbit IgG antibody (Molecular Probes, Eugene, OR, USA) and diluted to 1:2000 with blocking buffer for 1 hr at room temperature. After a final wash, the cells were stained with DAPI and viewed under an immunofluorescence microscope (IX71N-22PH; Olympus, Tokyo, Japan).

In some experiments, after the irradiation of UV-B, the cultures were treated with p38 inhibitor (SB203580). Then, the cell/matrix layers were incubated for 2 hr with anti-human phospho-p38 mitogen-activated protein kinase

(MAPK) polyclonal antibody (#9211: Cell Signaling Technology) and diluted to 1:2000 with blocking buffer for 1 hr at room temperature. After being rinsed in PBS, the cells were incubated with Alexa Fluor 568-labeled goat anti-rabbit IgG antibody (Molecular Probes, USA) and diluted to 1:2000 with blocking buffer for 1 hr at room temperature. After a final wash, the cells were viewed as described above.

MMP-2 ELISA assay

A human MMP-2 ELISA kit (QuickZyme Biosciences, Leiden, Netherland) was used to measure the protein level of both active-type MMP-2 and total MMP-2 in the cell/matrix of the culture. In brief, at 12 and 24 hr after UV irradiation, cell/matrix samples from two 60-mm plastic culture dishes were homogenized with TBS containing 0.1% Triton-X 100 (v/v) and centrifuged at $10,000 \times g$ for a minimum of 10 min, to remove any cell/matrix debris. A monoclonal antibody specific for MMP-2 was pre-coated onto a microplate. Standards and appropriate diluted samples were pipetted into the wells. Following the incubation, unbound samples were removed by washing, and then samples were activated by p-aminophenyl mercuric acetate (APMA) for the detection of total MMP-2. Following washing to remove any unbound components, enzyme conjugate was added to the wells. Following incubation and washing, the substrate was added. A colored product is formed in proportion to the amount of MMP-2 present in the sample. The reaction was terminated by the addition of acid, and absorbance was measured at 405 nm. A standard curve was prepared from 13 MMP-2 standard dilutions, and the MMP-2 sample concentration was determined. For the detection of active-type MMP-2, the same procedure was performed without APMA treatment.

Western blot analysis

After 24 hr of UV irradiation, cell/matrix samples from two 60-mm plastic culture dishes were mixed with 10 mM Tris-HCl, pH 8.0/150 mM NaCl (TBS) and homogenized. Then, homogenized samples (20 μl) were mixed with 20 μl of 2 × gel electrophoresis loading buffer (Tris-Glycine SDS) containing 2-mercaptoethanol (4 μl) (Wako Pure Chemicals, Osaka, Japan) and boiled at 100°C for 3 min. The above samples (20 μl) were run on 5%–20% polyacrylamide gel (ATTO, Tokyo, Japan). The electrophoresed proteins were transferred to Immobilon-P (Merck Millipore, Tullgren, Carrigtwohill, Ireland) in a tank blotter in 25 mM Tris / 192 mM glycine, pH 8.3, at 15 V for 2 hr. The Immobilon-P were blocked with 4% non-fat skim milk in 10 mM Tris-HCl, pH 8.0 / 150 mM NaCl/ 0.05% Tween-20 (TBST) for 2 hr and then incubated with anti-human p38 MAPK polyclonal antibody (#9212; Cell Signaling Technology), anti-human phospho-p38 MAPK polyclonal antibody (#9211; Cell Signaling Technology), or anti-human β-actin monoclonal antibody (#4970; Cell Signaling Technology) at a dilution of 1:2000 for 2 hr. The Immobilon-P were washed three times with TBST and then incubated with anti-rabbit IgG HRP-linked antibody (#7074; Cell Signaling Technology) at a dilution of 1:2000 with TBST for 1 hr.

Data analysis

All quantitative data are shown as means ± standard deviation (SD). Quantitative analysis was made using a one-way ANOVA model and the Tukey-Kramer test. Differences with P values of less than 0.05 were considered statistically significant.

III. Results

Under control culture conditions (0 mJ/cm^2), continuous fibrillin-1- and fibrillin-2-positive fibers were observed throughout the culture dish. As we reported previously [25], the fibrillin-1-positive fibers became thin, and their continuity disappeared after UV-B irradiation at 100 mJ/cm^2. In addition, fibrillin-2-positive fibers showed a decrease in positivity and disappeared at an irradiation level of 100 mJ/cm^2 (Fig. 1).

Next, in order to calculate the involvement of MMP-2 in the UV-B-induced degradation of oxytalan fibers, we quantified the level of MMP-2 in the cell/matrix at 12 and 24 hr after UV-B irradiation using ELISA. At 12 hr, the levels of total MMP-2 at an irradiation level of 150 mJ/cm^2 were increased 1.7 times compared with the control (0 mJ/cm^2). The levels of active MMP-2 at an irradiation level of 150 mJ/cm^2 were increased 2.2 times compared with control (Fig. 2A). Similarly, the significant increases in total and active MMP-2 levels by UV-B irradiation were observed at 24 hr (Fig. 2B). No detectable amount of MMP-2 was observed in culture media containing 10% serum (data not shown), reflecting the secretion of MMP-2 by HNPCEC.

Next, we investigated whether UV-B-increased MMP-2 is involved in the degradation of fibrillin-1 and fibrillin-2 using two reagents which inhibit MMP-2 and MMP-2/MMP-9. As shown in Figures 3 and 4, the addition of MMP-2 inhibitor (Fig. 3) and MMP-2/MMP-9 inhibitor (Fig. 4) suppressed the UV-B-induced degradation of oxytalan fibers, whereas the vehicle control did not (Fig. 5). These results suggest that at least MMP-2 degrades fibers positive for fibrillin-1 and fibrillin-2.

Next, we explored how UV-B irradiation increases MMP-2 levels. Here we focused on MAPK p38, because researchers reported that mechanical force stimulates MMP-2 expression via the p38 pathway in human retinal pigment epithelial cells [9] and that UV simulates the p38 pathway in mammalian cells [6, 14, 24]. Western blot revealed that phosphorylated p38 clearly appeared after 5 min and peaked at 10 min (Fig. 6A). Since it is reported that the phosphorylated p38 upon UV-B irradiation is accumulated in nuclei [27], the localization of phosphorylated p38 was analyzed by immunofluorescence staining. In line
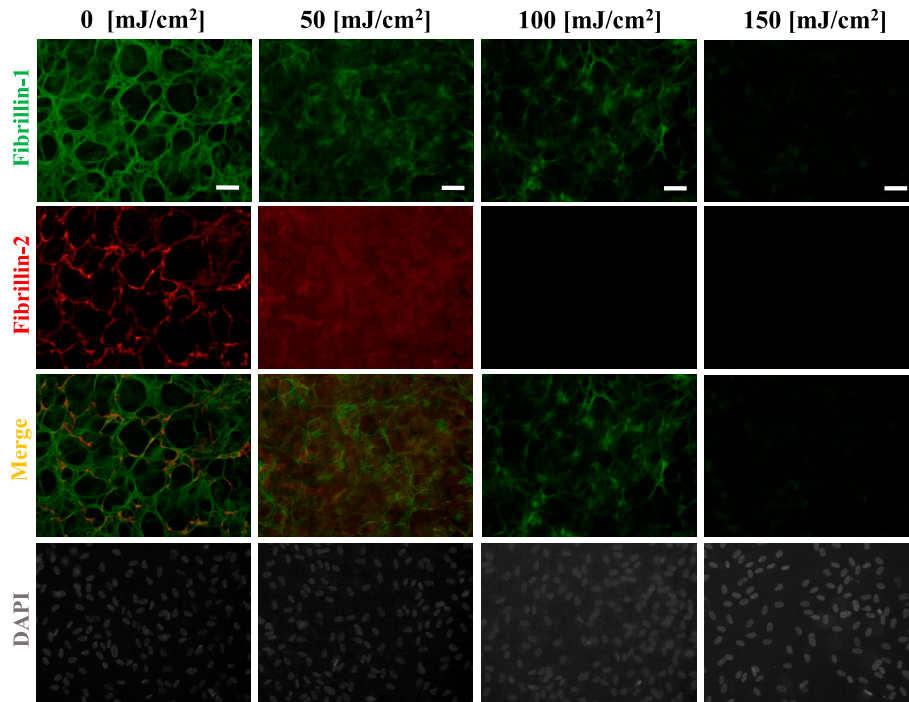
Fig. 1. Degradation of fibrillin-1 and fibrillin-2 by UV-B irradiation. Double immunofluorescence for fibrillin-1 (upper first panels) and fibrillin-2 (second panels) in cultures of human nonpigmented ciliary epithelial cells. The cells were irradiated with the indicated dose of UV-B irradiation and then cultured for 24 hr, and doubly labeled for fibrillin-1 (green; first panels) and fibrillin-2 (red; second panels). Superimposition of both labels is shown in the third panels. DAPI for nuclear staining is shown in the fourth panels. Fibrillin-1-positive oxytalan fibers disappeared at a UV-B irradiation level of 150 mJ/cm^2 and fibrillin-2-positive oxytalan fibers disappeared at a UV-B irradiation level of 100 mJ/cm^2 and higher. Bar = 50 μm.
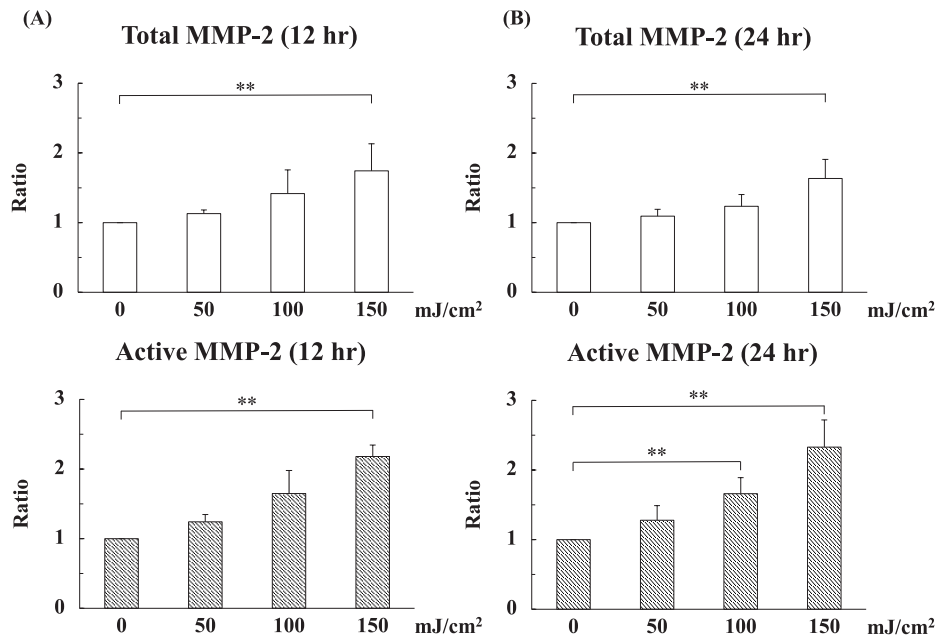

Fig. 2. UV-B irradiation increased matrix metalloproteinase-2 (MMP-2) in cell lysates. Human nonpigmented ciliary epithelial cells were cultured for 4 weeks and then irradiated with UV-B at levels of 0, 50, 100, and 150 mJ/cm^2. Then, the cells were cultured for another 24 hr under the same culture conditions. Next, cell/matrix layers were collected at 12 (**A**) and 24 (**B**) hr after UV irradiation and analyzed by ELISA. The level of active MMP-2 increased depending on the irradiation level of UV-B. (**A**) The levels of total and active MMP-2 at 150 mJ/cm^2 were significantly increased compared to the control (0 mJ/cm^2). (**A**) The levels of total and active MMP-2 at 100 and 150 mJ/cm^2 were significantly increased compared to the control (0 mJ/cm^2). (**B**) The level of active MMP-2 at 100 mJ/cm^2 were significantly increased compared to the control (0 mJ/cm^2). The amounts of total and active MMP-2 at 150 mJ/cm^2 were significantly increased compared to the control (0 mJ/cm^2). The values for each control sample (0 mJ/cm^2) were arbitrarily assigned a value of 1. The results represent the mean ± standard deviation of four independent determinations. **$P < 0.05$ versus control.
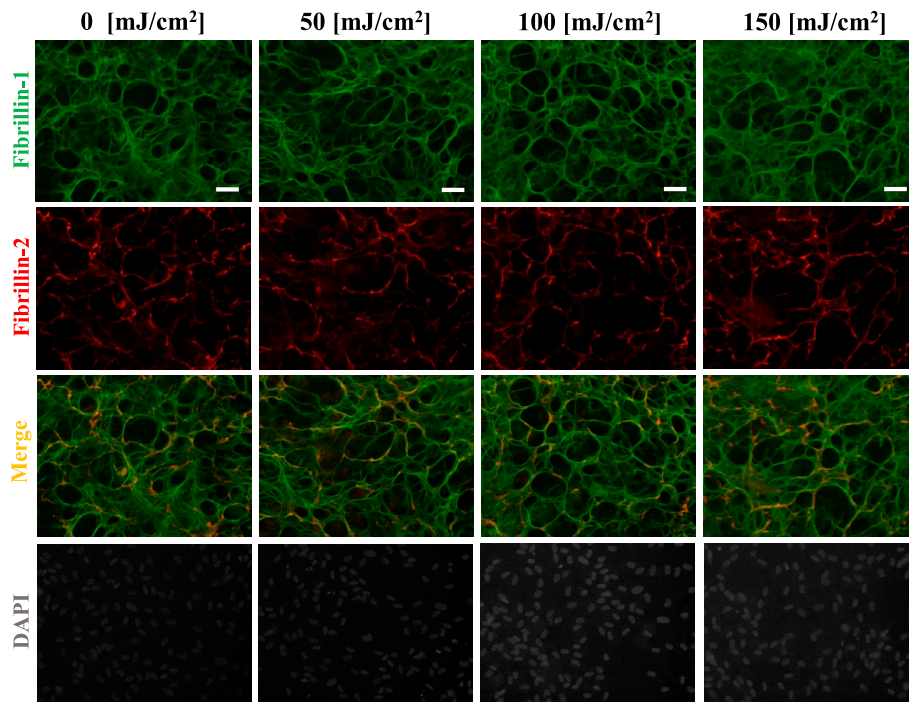
Fig. 3. Inhibitory effect by addition of MMP-2 inhibitor. Human nonpigmented ciliary epithelial cells were cultured for 4 weeks and then irradiated with UV-B at levels of 0, 50, 100, and 150 mJ/cm². Then, 1.5 μM MMP-2 inhibitor was added to the medium for an additional 24 hr. After 24 hr, the cells were simultaneously labeled for fibrillin-1 (green; first panels) and fibrillin-2 (red; second panels). Superimposition of both labels is shown in the third panels. DAPI for nuclear staining is shown in the fourth panels. Bar = 50 μm.
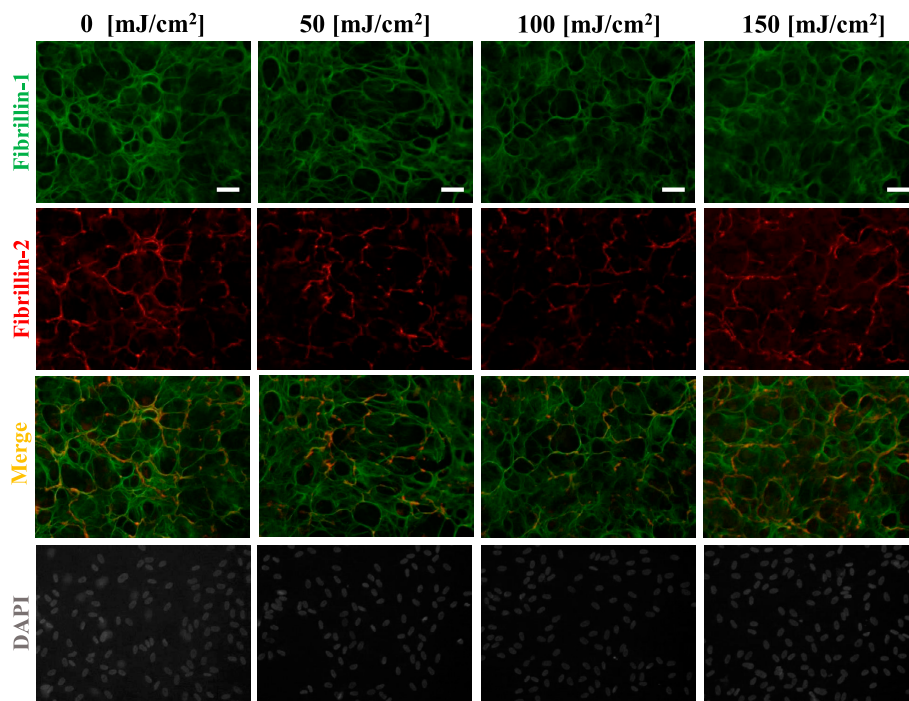

Fig. 4. Inhibitory effect by addition of MMP-2/MMP-9 inhibitor. Human nonpigmented ciliary epithelial cells were cultured for 4 weeks and then irradiated with UV-B at levels of 0, 50, 100, and 150 mJ/cm². Then, 50 nM MMP-2/MMP-9 inhibitor was added to the medium for an additional 24 hr. After 24 hr, the cells were doubly labeled for fibrillin-1 (green; first panels) and fibrillin-2 (red; second panels). Superimposition of both labels is shown in the third panels. DAPI for nuclear staining is shown in the fourth panels. Bar = 50 μm.
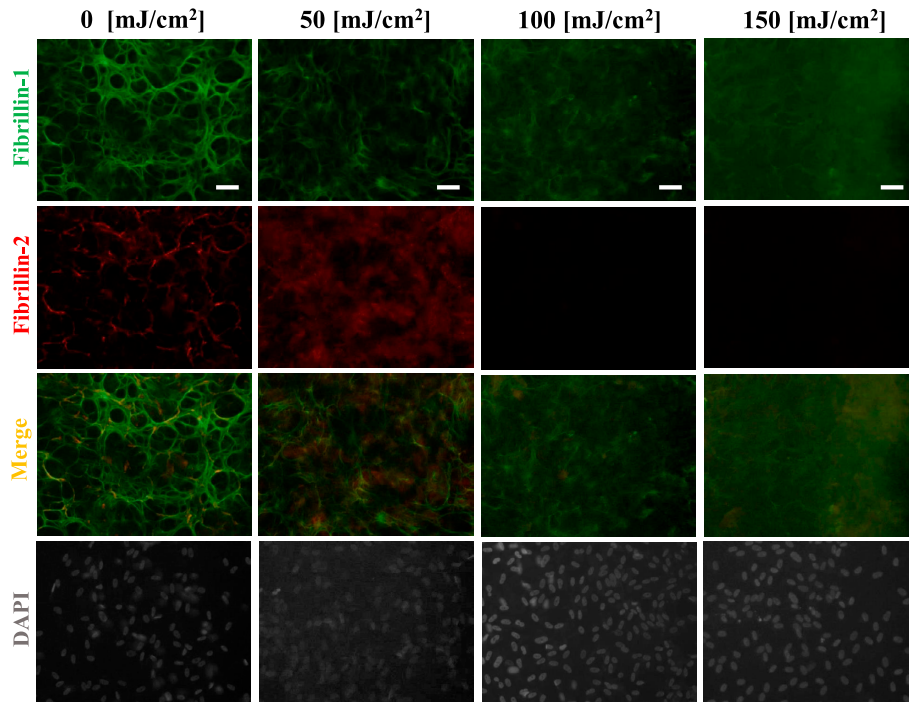
Fig. 5. Negative control for the effect of MMP inhibitors. Human nonpigmented ciliary epithelial cells were cultured for 4 weeks and then irradiated with UV-B at levels of 0, 50, 100, and 150 mJ/cm^2. Then, DMSO at an equivalent concentration (0.01%) as in Figures 3 and 4 in DMEM with 10% serum was added to the medium for an additional 24 hr. After 24 hr, the cells were doubly labeled for fibrillin-1 (green; first panels) and fibrillin-2 (red; second panels). Superimposition of both labels is shown in the third panels. DAPI for nuclear staining is shown in the fourth panels. Bar = 50 μm.
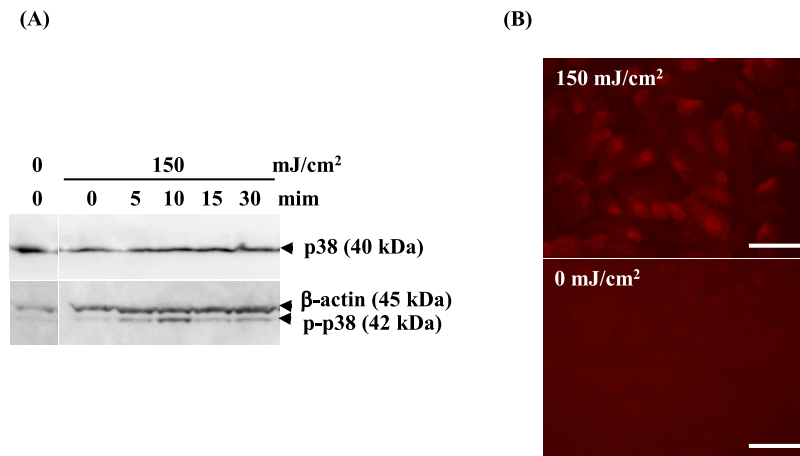

Fig. 6. UV-B irradiation at 150 mJ/cm^2 induced p38 activation. (**A**) Human nonpigmented ciliary epithelial cells were cultured for 24 hr and then irradiated with UV-B at a level of 150 mJ/cm^2. The cell/matrix layers were collected at 0, 5, 10, 15, and 30 min after UV irradiation and analyzed by Western blot against p38 and phosphor-p38. The protein levels of p38 did not change, whereas those of phosphor-p38 were maximally detected at 10 min. (**B**) 10 min after irradiation, the cells were labeled for phosphor-p38. Phospho-p38 is labeled in the nucleus at 150 mJ/cm^2, whereas it is not labeled at 0 mJ/cm^2. Bar = 50 μm.

with the results of Western blotting, immunofluorescence staining indicated the high expression of phosphorylated p38 in the nucleus, not in the cytoplasmic region, 10 min after UV-B irradiation (Fig. 6B). These results suggest that UV-B increased the expression of phosphorylated p38 in

HNPCEC. Finally, we examined whether inhibition of p38 activation can affect MMP-2 secretion after UV-B irradiation. As shown in Fig. 7A–C, the p38 inhibitor, SB203580, clearly inhibited the production of UV-B-increased active MMP-2 (Fig. 7C), as well as the expression of phosphory-
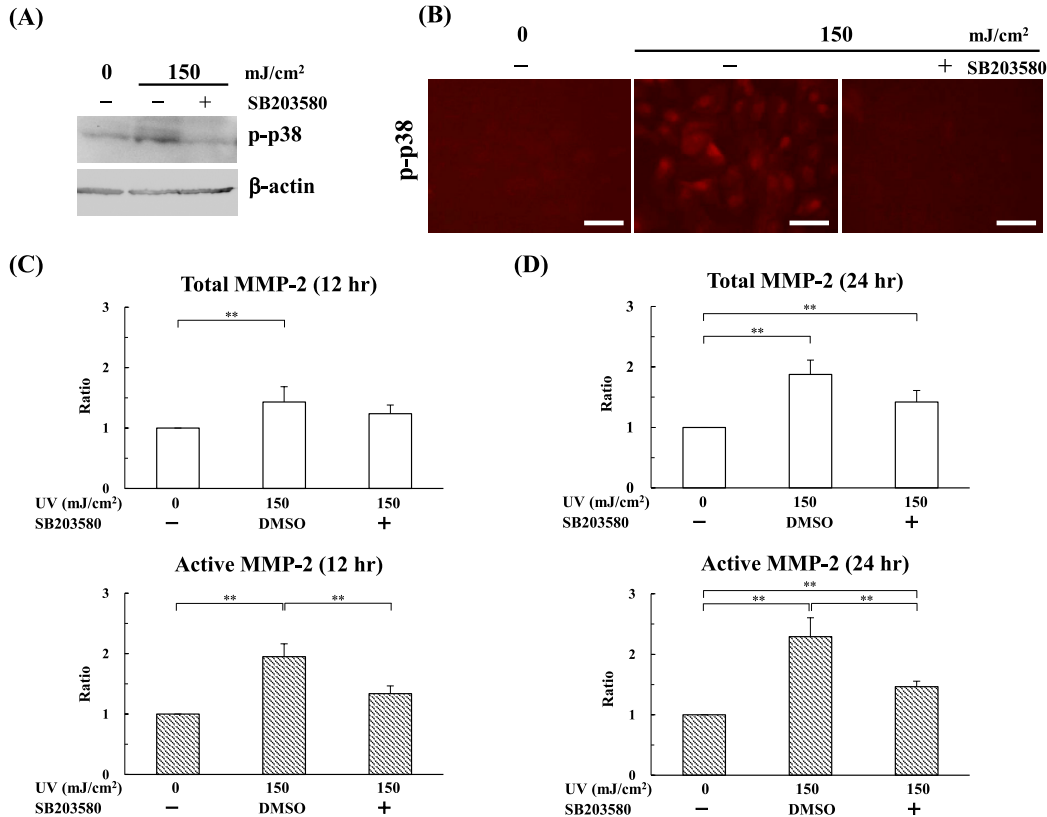
Fig. 7. UV-B irradiation increases the level of MMP-2 via p38 activation. Human nonpigmented ciliary epithelial cells were cultured for 24 hr and then the cells pretreated with SB203580 (p38 inhibitor) were irradiated with UV-B at levels of 0, 50, 100, and 150 mJ/cm². Then, the cells were cultured for another 12 and 24 hr under serum-free culture conditions. (**A**) Cell/matrix layers were collected 10 min after UV irradiation and analyzed by Western blot against phosphor-p38. The level of phosphor-p38 treated with SB203580 was inhibited at the same level as the control (0 mJ/cm²). (**B**) Immunofluorescence showed that phosphor-p38 was labeled in the cells at 150 mJ/cm², but not in SB203580-treated cells. Cell/matrix layers were collected at 12 (**C**) and 24 (**D**) hours after UV irradiation and analyzed by ELISA. The active MMP-2 in the SB203580-treated cells was suppressed compared with the SB203580-untreated vehicle cells. The values for each control sample (0 mJ/cm²) without SB203580 were arbitrarily assigned a value of 1. The results represent the mean ± standard deviation of four independent determinations. **$P < 0.05$ versus control.

lated p38 (Fig. 7A and 7B). Treatment with SB203580 did not confer any effect on total and active MMP-2 at the level of 0 mJ/cm² (data not shown). These results show that UV-B increases the active MMP-2 level in a p38-dependent manner.

IV. Discussion

We previously demonstrated that fibrillin-1 and fibrillin-2 in HNPCEC culture were degraded after UV-B irradiation, but not after UV-A irradiation [25]. However, how UV-B irradiation degrades fibrillin-1 and fibrillin-2 remains unclear. In this study, we found that UV-B irradiation significantly activated MMP-2 in HNPCEC culture and that MMP-2 inhibitors suppressed the degradation of fibrillin-1 and fibrillin-2 after UV-B irradiation. These results demonstrate for the first time that UV-B irradiation degrades oxytalan fibers positive for fibrillin-1 and fibrillin-2 in HNPCEC culture through MMP-2.

In the human body, the effects of UV-B on MMP-2 induction in the eye is not well-known. However, in terms of adjacent tissues of the ciliary zonules, researchers reported that UV-B inducts MMP-2 expression in human corneal fibroblasts, but not human corneal epithelial cells [13]. In the previous study, human corneal fibroblasts were irradiated with 0, 80, 160, 320, and 480 mJ/cm² UV-B, and the peak of MMP-2 expression was observed at 160 mJ/cm². In the present study, we showed that a similar UV-B irradiation level (i.e., 150 mJ/cm²) increased MMP-2 expression in HNPCEC culture. These results suggest that UV-B irradiation can induce MMP-2 in some types of cell in the eye. Since the UV-B irradiation level tested in this study may be higher than a chronic exposure to environmental UV, further investigations using similar UV level to environmental UV exposure are needed.

Fibrillin-1 and fibrillin-2 are molecules of approximately 350 kDa and exhibit similar structures; however, the homologous region near the amino termini is proline-rich in fibrillin-1, whereas it is glycine-rich in fibrillin-2 [23, 28]. The majority of the structure is the epidermal growth factor (EGF)-like domain. The EGF-like domain binds calcium to stabilize against MMPs [19]. In general, it is known that

physiological remodeling of elastic system fibers, including ciliary zonules, is very slow during human life [20], and the degradation pattern of ciliary zonules during aging is not yet known. HNPCEC were reported to express mRNA and the protein MMP-1, -2, -3, and -9 [8]. Among these MMPs, researchers reported that fibrillin-1 is a substrate for MMP-2, -3, and -9, and fibrillin-2 is a substrate for MMP-2 and -9, by *in vitro* examination using peptides from ciliary zonules [1, 7]. The present results strongly indicate the involvement of MMP-2 in the UV-B-induced degradation of oxytalan fibers. However, since the MMP-2/MMP-9 inhibitor used in this study also suppressed the degradation of oxytalan fibers positive for fibrillin-1 and fibrillin-2, the possibility exists that not only MMP-2 but also MMP-9 is involved in the UV-B-induced degradation of oxytalan fibers. To clarify this possibility, further studies focusing on MMP-9 are needed.

p38 MAPK is a well-known stress-responsive kinase, and it plays a crucial role in the regulation of cellular responses, such as gene expression and apoptosis [10]. Recently, Kwon *et al.* demonstrated that human keratinocyte cells irradiated with 40 mJ/cm^2 UV-B showed p38 activation, which leads to MMP-2 expression [14]. In line with their report, we found that p38 plays a key role in the UV-B-induced activation of MMP2 in HNPCEC culture. Although the present study did not investigate how UV-B activates the p38 pathway, researchers reported that reactive oxygen species mediate the activation of p38 by UV-B irradiation in keratinocytes [17]. Therefore, it is likely that UV-B activates the p38 pathway through reactive oxygen species in HNPCEC.

Also, human hepatocellular carcinoma cells which are stimulated with Genipin, a metabolite of geniposide, show downregulations of expression of tissue inhibitor of metalloproteinase (TIMP)-1 and upregulations of expression of MMP-2 via p38 signaling pathway [26]. We cannot deny the possibility that TIMP-1 affects the activation of MMP-2 in our experiment. Further studies are necessary to delineate this issue.

Anatomically, a UV reaches to the ciliary body through cornea, pupil, and aqueous humor. Meanwhile, the cornel endothelial cells, fibroblasts and keratinocytes are exposed to the UV. Described above, human corneal fibroblasts express MMP-2 [13] and human keratinocyte also express MMP-2 [14] after irradiation of UV-B *in vitro*. Therefore, further studies are necessary to elucidate the effect of MMP-2 at the adjacent area of ciliary body by reflux manner on the degradation of ciliary zonules.

In conclusion, our *in vitro* study suggests that UV-B activates MMP-2 via the p38 pathway, which results in the degradation of fibrillin-1- and fibrillin-2 in the ciliary zonules. Although no available data exist to suggest that ciliary zonules and HNPCEC are exposed to UV light *in vivo*, Sachdev *et al.* suggested a possibility that UV reaches the HNPCEC on the ciliary body [22]. Anatomically, some incidental UV-B should proceed through the cornea and aqueous humor and reach the ciliary zonule and HNPCEC on the ciliary body. Therefore, although the conditions may differ *in vivo* and *in vitro*, we believe that our findings may help to explain the homeostasis of the ciliary zonule during aging.

V.   Conflicts of Interest

The authors declare that there are no conflicts of interest.

VI.   References

1. Ashworth, J. L., Kelly, V., Rock, M. J., Shuttleworth, C. A. and Kielty, C. M. (1999) Regulation of fibrillin carboxy-terminal furin processing by N-glycosylation, and association of amino- and carboxy-terminal sequences. *J. Cell Sci.* 112; 4163–4171.
2. Baldock, C., Koster, A. J., Ziese, U., Rock, M. J., Sherratt, M. J., Kadler, K. E., *et al.* (2001) The supramolecular organization of fibrillin-rich microfibrils. *J. Cell Biol.* 152; 1045–1056.
3. Dechow, T. N., Pedranzini, L., Leitch, A., Leslie, K., Gerald, W. L., Linkov, I., *et al.* (2004) Requirement of matrix metalloproteinase-9 for the transformation of human mammary epithelial cells by Stat3-C. *Proc. Natl. Acad. Sci. U S A* 101; 10602–10607.
4. De Maria, A., Wilmarth, P. A., David, L. L. and Bassnett, S. (2017) Proteomic analysis of the bovine and Human ciliary zonule. *Invest. Ophthalmol. Vis. Sci.* 58; 573–585.
5. Fullmer, H. M. and Lillie, R. D. (1958) The oxytalan fiber: a previously undescribed connective tissue fiber. *J. Histochem. Cytochem.* 6; 425–430.
6. Gong, X., Liu, A., Ming, X., Deng, P. and Jiang, Y. (2010) UV-induced interaction between p38 MAPK and p53 serves as a molecular switch in determining cell fate. *FEBS Lett.* 584; 4711–4716.
7. Hindson, V. J., Ashworth, J. L., Rock, M. J., Cunliffe, S., Shuttleworth, C. A. and Kielty, C. M. (1999) Fibrillin degradation by matrix metalloproteinases: identification of amino- and carboxy-terminal cleavage sites. *FEBS Lett.* 452; 195–198.
8. Hinz, B., Rösch, S., Ramer, R., Tamm, E. R. and Brune, K. (2005) Latanoprost induces matrix metalloproteinase-1 expression in human nonpigmented ciliary epithelial cells through a cyclooxygenase-2-dependent mechanism. *FASEB J.* 19; 1929–1931.
9. Hou, X., Han, Q. H., Hu, D., Tian, L., Guo, C. M., Du, H. J., *et al.* (2009) Mechanical force enhances MMP-2 activation via p38 signaling pathway in human retinal pigment epithelial cells. *Graefes Arch. Clin. Exp. Ophthalmol.* 247; 1477–1486.
10. Johnson, G. L. and Lapadat, R. (2002) Mitogen-activated protein kinase pathways mediated by ERK, JNK, and p38 protein kinases. *Science* 298; 1911–1912.
11. Kawagoe, M., Tsuruga, E., Oka, K., Sawa, Y. and Ishikawa, H. (2013) Matrix metalloproteinase-2 degrades fibrillin-1 and fibrillin-2 of oxytalan fibers in the human eye and periodontal ligaments in vitro. *Acta Histochem. Cytochem.* 46; 153–159.
12. Kawano, S., Takeuchi, M., Tanaka, S., Yamashita, T., Sakamoto, T. and Kawakami, K. (2019) Current status of late and recurrent intraocular lens dislocation: analysis of real-world data in Japan. *Jpn. J. Ophthalmol.* 63; 65–72.
13. Koźák, I., Klisenbauer, D. and Juhás, T. (2003) UV-B induced production of MMP-2 and MMP-9 in human corneal cells. *Physiol. Res.* 52; 229–234.

14. Kwon, K. R., Alam, M. B., Park, J. H., Kim, T. H. and Lee, S. H. (2019) Attenuation of UVB-induced photo-aging by polyphenolic-rich Spatholobus Suberectus Stem extract via modulation of MAPK/AP-1/MMPs signaling in human keratinocytes. *Nutrients* 11; 1341.

15. Mecham, R. P. and Davis, E. C. (1994) Elastic fiber structure and assembly. In "Extracellular Matrix Assembly and Structure" ed. by P. D. Yurchenco, D. E. Birk and R. P. Mecham, Academic Press, New York, pp. 281–314.

16. Niimura, Y., Moue, T., Takahashi, N. and Nagai, K. (2008) Screening of biomarker genes activated by irradiation of ultraviolet B rays in mouse lymph node M10 cells. *J. Radiat. Res.* 49; 635–644.

17. Peus, D., Vasa, R. A., Beyerle, A., Meves, A., Krautmacher, C. and Pittelkow, M. R. (1999) UVB activates ERK1/2 and p38 signaling pathways via reactive oxygen species in cultured keratinocytes. *J. Invest. Dermatol.* 112; 751–756.

18. Raviola, G. (1971) The fine structure of the ciliary zonule and ciliary epithelium. With special regard to the organization and insertion of the zonular fibrils. *Invest. Ophthalmol.* 10; 851–869.

19. Reinhardt, D. P., Mechling, D. E., Boswell, B. A., Keene, D. R., Sakai, L. Y. and Bächinger, H. P. (1997) Calcium determines the shape of fibrillin. *J. Biol. Chem.* 272; 7368–7373.

20. Rosenbloom, J., Abrams, W. R. and Mecham, R. (1993) Extracellular matrix 4: the elastic fiber. *FASEB J.* 7; 1208–1218.

21. Rossello, A., Nuti, E., Orlandini, E., Carelli, P., Rapposelli, S., Macchia, M., *et al.* (2004) New N-arylsulfonyl-N-alkoxyaminoacetohydroxamic acids as selective inhibitors of gelatinase A (MMP-2). *Bioorg. Med. Chem.* 12; 2441–2450.

22. Sachdev, N., Wakefield, D. and Coroneo, M. T. (2003) Lens dislocation in Marfan syndrome and UV-B light exposure. *Arch. Ophthalmol.* 121; 585.

23. Sakai, L. Y., Keene, D. R. and Engvall, E. (1986) Fibrillin, a new 350-kD glycoprotein, is a component of extracellular microfibrils. *J. Cell Biol.* 103; 2499–2509.

24. She, Q. B., Chen, N. and Dong, Z. (2000) ERKs and p38 kinase phosphorylate p53 protein at serine 15 in response to UV radiation. *J. Biol. Chem.* 275; 20444–20449.

25. Shiroto, Y., Terashima, S., Hosokawa, Y., Oka, K., Isokawa, K. and Tsuruga, E. (2017) The effect of ultraviolet B on fibrillin-1 and fibrillin-2 in human non-pigmented ciliary epithelial cells in vitro. *Acta Histochem. Cytochem.* 50; 105–109.

26. Wang, N., Zhu, M., Tsao, S. W., Man, K., Zhang, Z. and Feng, Y. (2012) Up-regulation of TIMP-1 by genipin inhibits MMP-2 activities and suppresses the metastatic potential of human hepatocellular carcinoma. *PLoS One* 7; e46318.

27. Wood, C. D., Thornton, T. M., Sabio, G., Davis, R. A. and Rincon, M. (2009) Nuclear localization of p38 MAPK in response to DNA damage. *Int. J. Biol. Sci.* 5; 428–437.

28. Zhang, H., Apfelroth, S. D., Hu, W., Davis, E. C., Sanguineti, C., Bonadio, J., Mecham, R. P., *et al.* (1994) Structure and expression of fibrillin-2, a novel microfibrillar component preferentially located in elastic matrices. *J. Cell Biol.* 124; 855–863.

29. Zhang, H., Hu, W. and Ramirez, F. (1995) Developmental expression of fibrillin genes suggests heterogeneity of extracellular microfibrils. *J. Cell Biol.* 129; 1165–1176.